4.4 FABRICATION OF FUNCTIONALLY GRADED TUNGSTEN STEEL LAMINATE—L. M. Garrison, Y. Katoh (Oak Ridge National Laboratory), M. Norfolk (Fabrisonic LLC.), J. Wenning (Fabrisonic LLC.), J. Moon (University of Nevada-Reno)

OBJECTIVE

The objective of this project is to create a functionally graded tungsten to steel laminate composite for use in plasma facing components in fusion reactors.

SUMMARY

Two roll-bonded tungsten-steel composites have been fabricated. Tensile tests of the Generation 2 composite were completed and showed increasing strength and decreasing ductility with increased tungsten content. A feasibility study for ultrasonic welding tungsten to steel was completed. Thirty-four trials were completed that varied the parameters of foil thickness, interlayer material, welding force, vibration amplitude, and other welding parameters. Promising results were obtained for joining tungsten to steel and tungsten to steel with an aluminum interlayer.

PROGRESS AND STATUS

Introduction

For the plasma-facing components of fusion reactors, tungsten will be the interface between the plasma and the underlying structural component because tungsten has a low sputtering yield, high melting temperature, and relatively high thermal conductivity. However, because tungsten is brittle and has low fracture toughness, it is impractical to fabricate the entire plasma-facing component out of tungsten. Current divertor designs utilize various methods to bond the tungsten surface layer to the underlying structural part of the component that contains the cooling channels, but for future divertors where the operating temperature will be higher, more robust solutions are needed. Advanced steels are being developed for structural components in future fusion reactors. Unfortunately, tungsten and steel have vastly different coefficients of thermal expansion, so a direct joint would be subjected to intense thermal stresses. A tungsten-steel functionally graded material would ideally both improve the fracture toughness as compared to tungsten alone as well as reduce the thermal stresses between the tungsten and steel parts of the plasma-facing component.

Results

<u>Roll-bonding</u>
The Generation 1 laminate composite was fabricated by forging and hot rolling the tungsten and grade 92 steel foils within a stainless steel outer shell at 1000°C to 80% total thickness reduction overall. Tensile bars were machined from the Generation 1 composite. Because the composite has positional variations, each tensile bar must be characterized individually to count the number of layers included and the thickness of the layers. This characterization is underway and will be followed by tensile and shear punch tests.

The Generation 2 composite was fabricated using ten layers of 250 μm Grade 92 steel alternating with ten layers of 25 μm tungsten and was forged at 1000°C for only 20% thickness reduction. The goal of the Generation 2 composite is to determine if the processing parameters can be optimized to create bonding between the layers without causing fragmentation of the tungsten layers, as was seen in the Generation 1 composite.

As seen in Figure 1, in the as-fabricated state the Generation 2 laminate composite had a large outer layer of stainless steel and a small volume of composite material at the center. Tensile samples were machined from the composite with electro-discharge machining such that the tensile axis was aligned

with the rolling direction of the foils. Because of the low visual contrast between the central composite and the outer stainless steel material, tensile samples could not be precisely cut from the central composite material.

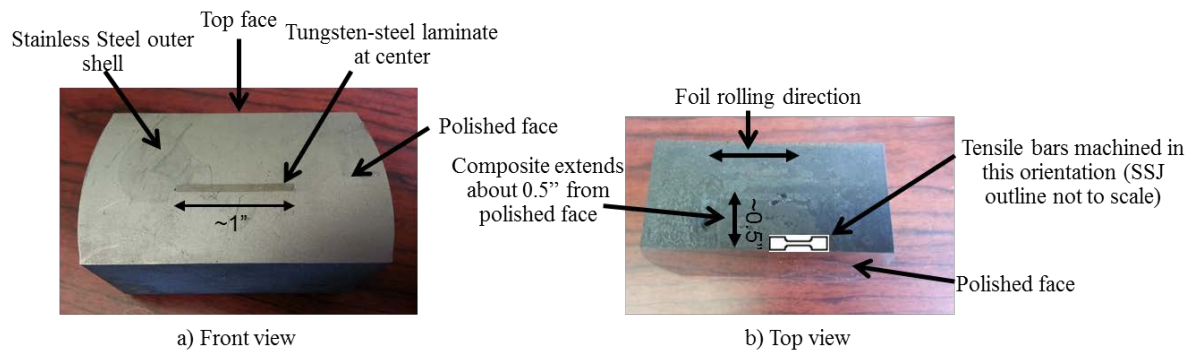

Figure 1. Generation 2 laminate composite. a) front view, showing composite inside stainless steel outer shell. b) top view.

Only one of the five samples tested (Figure 2), Sample A-1-1, showed evidence of containing the expected layers of both tungsten and Grade 92 steel (Figure 3). One other sample, Sample A-2-2, appeared to have a thin layer of tungsten on the outside of one face, as evidenced by a morphological difference characterized by shallow cracking perpendicular to the axis of the tensile load. Figure 2 illustrates that Sample A-1-1 is significantly stronger and more brittle than the three samples with no evidence of the layered composite, Samples A-1-2, A-2-1, and A-2-3. It is also apparent that Sample A-2-2 was stronger and less ductile than the three homogenous-appearing samples, but less strong and more ductile than Sample A-1-1. It may be reasonable to conclude that the continuum of increasing strength and decreasing ductility can be attributed to the difference in sample composition. Samples A-1-2, A-2-1 and A-2-3 appeared to be homogenous stainless steel of the outer shell and are the least strong and most ductile. Sample A-2-2 appeared to have some limited tungsten content and is stronger and less ductile than the homogenous-appearing samples. Sample A-1-1 has the expected, high level of tungsten layer content and is the strongest and least ductile. This pattern matches what would be expected based on the current understanding of the mechanical properties of these two materials. Further tensile tests of material from the Generation 2 composite are underway.

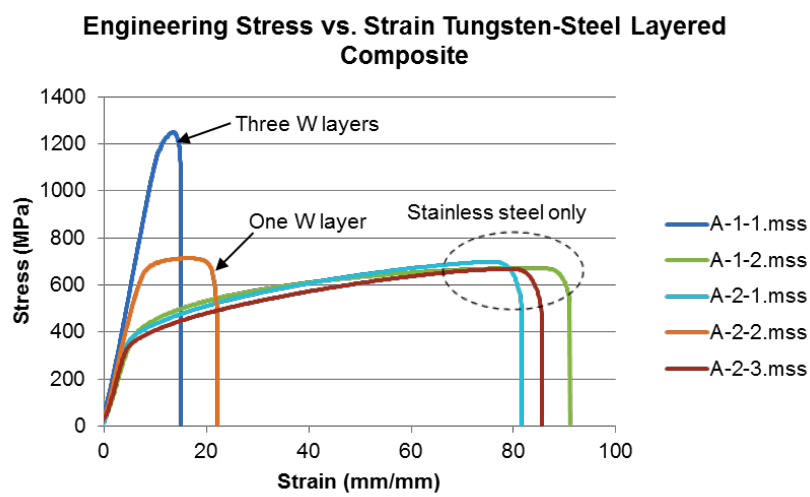

Figure 2. Stress-strain curves for composite material with three W layers, one W layer, and no W layers.

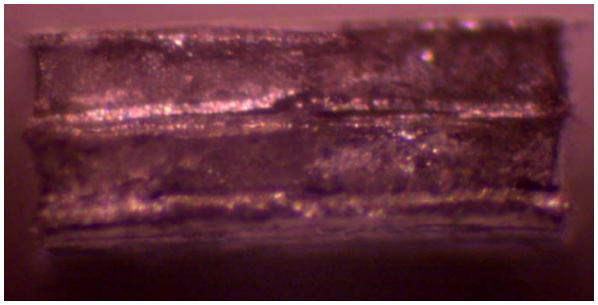

Figure 3. Fracture surface of composite Sample A-1-1 which contains three thin tungsten layers and two thicker steel layers. The height of the fracture end is approximately 0.5 mm.

Ultrasonic welding

An initial investigation of the feasibility of producing composites using ultrasonic bonding was completed with the company Fabrisonic, which specializes in ultrasonic welding of dissimilar materials. The ultrasonic welding process utilizes a sonotrode (also called a horn) that provides normal force onto the material to be bonded as well as side-to-side ultrasonic vibration (Figure 4). The combination of pressure and ultrasonic vibrations create a solid state bond between the layers. Material is built up one thin layer at a time to create a complete component. This lower temperature bonding strategy was considered for tungsten because other higher temperature bonding methods such as brazing or hot-rolling occur at temperatures where the tungsten is strong but the interlayer is usually very weak, and the different coefficients of thermal expansion of tungsten and candidate interlayers cause significantly different expansion of layers. These factors can lead to high residual stresses or non-uniform reduction in high-temperature processed tungsten composites. However, previous successful tungsten ultrasonic welds have not been reported in the literature, so this was a scoping study to evaluate the possibility of successfully welding tungsten to other candidate materials, especially steel and copper.

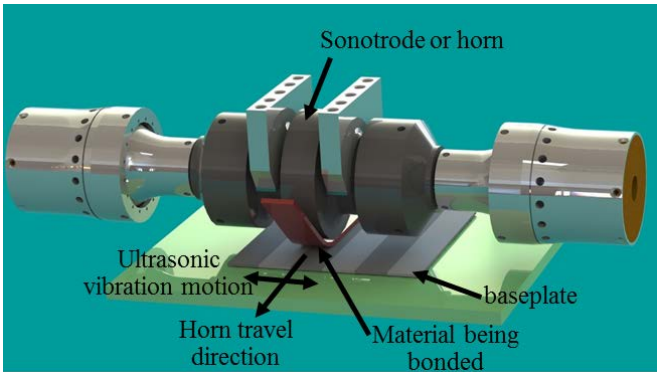

Figure 4. Image, adapted from http://fabrisonic.com/uam-overview/, shows the configuration of an ultrasonic welding device.

Two different baseplates were used in the trials, a C1020 carbon steel baseplate and an aluminum alloy 6061T6 baseplate. These two baseplates were chosen because they are frequently used at Fabrisonic and known to bond well with the trial interlayer materials of aluminum and copper. If feasibility of the tungsten ultrasonic welding could be shown, the baseplate could be replaced with a fusion specific alloy.

Three thicknesses of tungsten foils were used in the trials: 250 μm, 100 μm, and 25 μm thick. The outer dimensions of all the tungsten foils were one inch square. An important factor for the tungsten foils is their microstructure, which varies for each thickness of tungsten foil (Figure 5). The thickest foil had little grain orientation texture with somewhat elongated grains, while the thinnest foil had strong <100> texture

and small grains, and the medium thickness foil had intermediate properties. The general grain shape for the 100 µm and 25 µm foils was elongated along the rolling direction and thin in the cross section of the foil. The 250 25 µm foil had slightly more equiaxied grains than the thinner foils. One of the benefits of tungsten foils is that they can have delamination rather than brittle cleavage failure at room temperature. However, this is due to the weak grain boundaries moving against each other in response to stress.

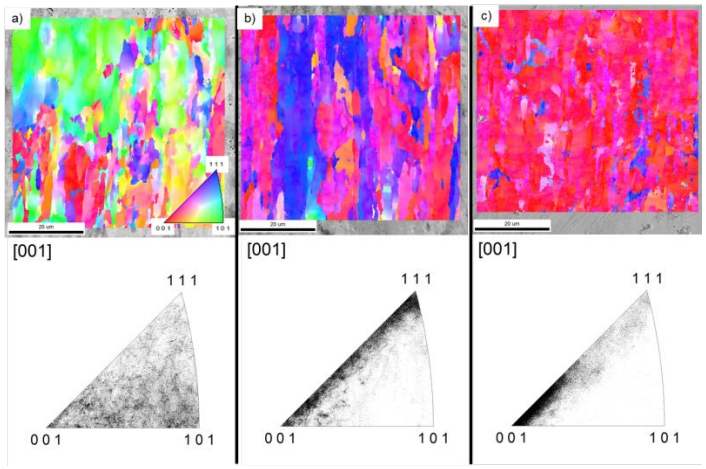

Figure 5. Electron backscatter diffraction images show the texture of tungsten foils of different thickness: a) 250 µm thick, b) 100 µm thick, and c) 50 µm thick.

The different tungsten microstructures caused the tungsten to behave differently during the ultrasonic welding. The 100 µm thick tungsten foil previously performed the best in the shear punch tests and in the hot-rolled tungsten steel composite. However, during trials of ultrasonically welding 100 µm thick tungsten foils, the foils had internal failure along the grain boundaries, which resulted in the foil delaminating into sub foils (Figure 6).

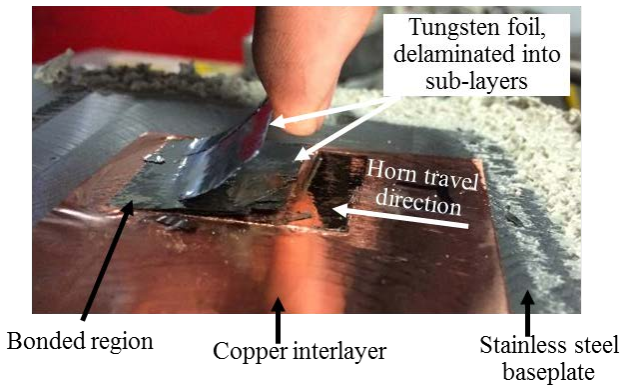

Figure 6. Welding trial of 100 µm thick tungsten foil with a 50 µm thick copper foil interlayer onto a C1020 carbon steel baseplate. The tungsten foil failed by internal delamination during the weld, but there was a bonded region at one end of the foil.

When the thinnest tungsten foil was used, it remained intact and did not fail by delamination as was seen for the 100 µm thick tungsten foil. The typical behavior for the 25 µm thick tungsten foil under various welding conditions was that the foil took on the texture of the sonotrode, showing good energy transfer and plastic deformation, but the foil did not bond to the copper interlayer. An example is shown in Figure 7 where a 25 µm thick tungsten foil lies to the side of the attempted weld region. The lack of bonding may be caused by failure to break through the surface oxide layer on the foil during welding or non-optimal welding parameters.

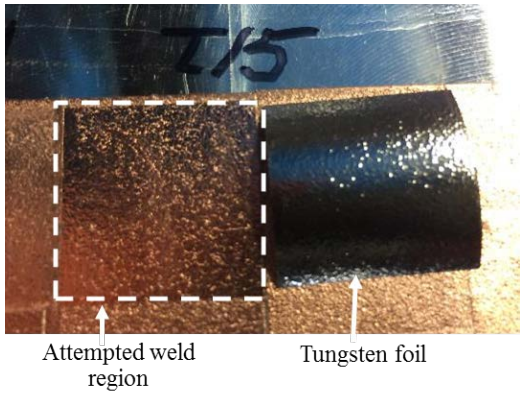

Figure 7. Weld trial using a 25 µm thick tungsten foil onto a copper interlayer on an aluminum alloy 6061T6 baseplate.

The 250 µm thick tungsten foil has less crystallographic texture than the thinner foils and in the previous shear punch test, it showed essentially no elongation. The different microstructure of the thickest tungsten foil manifested itself by shattering during many welding trials (example in Figure 8).

Figure 8. A tungsten foil, 250 µm thick cracked and shattered during a welding test with a copper interlayer and steel baseplate.

Overall, 34 trials were completed that varied the parameters of foil thickness, interlayer material, welding force, vibration amplitude, and other welding parameters. Success was achieved by lowering the normal force and adjusting the other welding parameters compared to the initial tests. Tungsten foils both 100 µm thick and 250 µm thick were able to be welded with minimal to no cracking in the tungsten layers (Figure 9). Welding parameters were developed for bonding tungsten foil to steel using an aluminum interlayer as well as separate parameters for directly bonding the tungsten foil to the steel baseplate. Further analysis will be completed on the successful weld trials including cross-sectional scanning electron microscopy to evaluate the phases and character at the bond interface. The initial investigation into ultrasonic welding of tungsten gathered important basic data on how the tungsten microstructure influences the weld and developed the general welding parameters necessary to weld tungsten to steel. The next step will be to determine if successive weld steps can be used to build a 3-D structure.

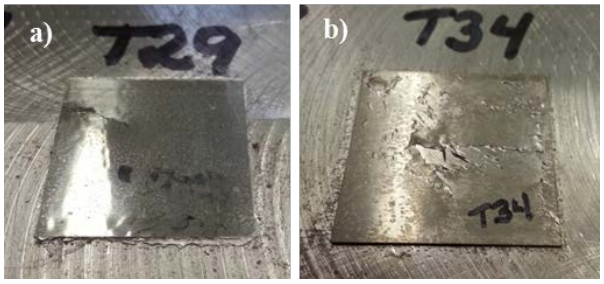

Figure 9. a) Bonding was achieved between a 100 µm thick tungsten foil, an 1100 aluminum interlayer, and a steel baseplate. b) direct bonding between a 250 µm thick tungsten foil and the steel baseplate.

Six of the trials that showed at least partial bonding success were selected for more in depth interface analysis. The welding trials were completed on large steel or aluminum base plates (Figure 10a). To prepare for interface analysis, small sub-sections of the selected trial joints were machined by electro-discharge machining, such as the example in Figure 10b. After machining, several sub-sections did not remain bonded, as in Figure 10c. The summary of which trials were selected for further analysis is in Table 1. Those that remained bonded will be examined with optical and scanning electron microscopy.

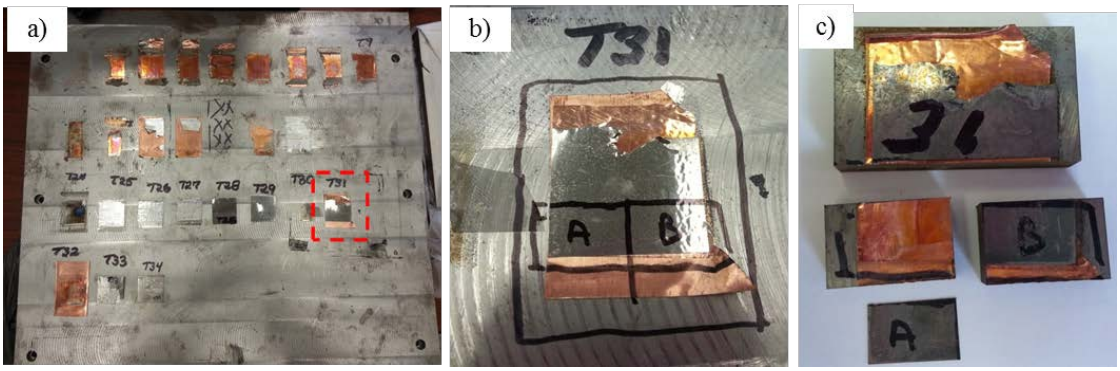

Figure 10. a) Steel baseplate with all ultrasonic weld trial locations. b) Trial 31 before sectioning. c) Trial 31 after sectioning.

Table 1. Ultrasonic welding trials selected for further interface analysis.

Trial number	W foil thickness	Interlayer	Substrate	Result after sectioning
23	0.025 mm	Cu	Al	Layers did not remain bonded
28	0.10 mm	Al	Steel	Layers remained bonded
29	0.10 mm	Al	Steel	One section remained bonded, one did not
31	0.10 mm	Cu	Steel	Layers did not remain bonded
33	0.25 mm	none	Steel	Both sections remained bonded
34	0.25 mm	none	Steel	One section remained bonded, one did not